Applied Energy 203 (2017) 115–127

Contents lists available at ScienceDirect

Applied Energy

journal homepage: www.elsevier.com/locate/apenergy

Frequency response services designed for energy storage

D.M. Greenwood [a,*], K.Y. Lim [b], C. Patsios [a], P.F. Lyons [a], Y.S. Lim [b], P.C. Taylor [a]

[a] School of Electrical and Electronic Engineering, Newcastle University, Newcastle upon Tyne NE1 7RU, UK
[b] Faculty of Engineering and Science, Universiti Tunku Abdul Rahman, Jalan Genting Klang, 53300 Kuala Lumpur, Malaysia

HIGHLIGHTS

- The need for improved frequency response in future power systems is identified.
- An investigation into how energy storage can fulfil this need is presented.
- New experimental methods have been developed, using power hardware in the loop.
- Analysis of high-resolution frequency data from the British electricity system.
- Case study analysis of a new frequency response service designed for energy storage.

ARTICLE INFO

Article history:
Received 23 February 2017
Received in revised form 27 May 2017
Accepted 11 June 2017
Available online 17 June 2017

Keywords:
Energy storage
Power systems
Frequency response
Hardware-in-the-loop
Real-time simulation

ABSTRACT

Energy Storage Systems (ESS) are expected to play a significant role in regulating the frequency of future electric power systems. Increased penetration of renewable generation, and reduction in the inertia provided by large synchronous generators, are likely to increase the severity and regularity of frequency events in synchronous AC power systems. By supplying or absorbing power in response to deviations from the nominal frequency and imbalances between supply and demand, the rapid response of ESS will provide a form of stability which cannot be matched by conventional network assets. However, the increased complexity of ESS operational requirements and design specifications introduces challenges when it comes to the realisation of their full potential through existing frequency response service markets: new service markets will need to be designed to take advantage of the capabilities of ESS. This paper provides new methods to analyse and assessing the performance of ESS within existing service frameworks, using real-time network simulation and power hardware in the loop. These methods can be used to introduce improvements in existing services and potentially create new ones. Novel statistical techniques have been devised to quantify the design and operational requirements of ESS providing frequency regulation services. These new techniques are demonstrated via an illustrative service design and high-resolution frequency data from the Great Britain transmission system.

1. Introduction

Frequency is a crucial parameter in an AC electric power system. Deviations from the nominal frequency are a consequence of imbalances between supply and demand; an excess of generation yields an increase in frequency, while an excess of demand results in a decrease in frequency [1]. The power mismatch is, in the first instance, balanced by changes in the kinetic energy stored within the rotating mass of large, synchronous generators. This response mitigates the effects of the imbalance, but does not correct it; that is the role of primary and secondary frequency response control of the power system. If the frequency deviates too far, statutory and operational limits will be breached, generators will be forced to disconnect, resulting in catastrophic failures within the system. The legal and operational limits for the GB (Great Britain) power systems are illustrated in Fig. 1.

In future power systems, the regularity and severity of frequency events is expected to increase as high penetrations of renewable generation lead to more variable, less predictable supply, and a reduction in system inertia as conventional plant is supplanted by renewable generators [2]. However, the advent of ESS creates an opportunity to provide frequency response significantly faster than the existing primary response; this can mitigate the increasing challenges in frequency control, and help enable higher penetrations of renewable energy.

Frequency Response (FR) is a necessary part of any AC power system, and is usually procured via ancillary service markets. The

* Corresponding author.
E-mail address: david.greenwood@ncl.ac.uk (D.M. Greenwood).

http://dx.doi.org/10.1016/j.apenergy.2017.06.046
0306-2619/

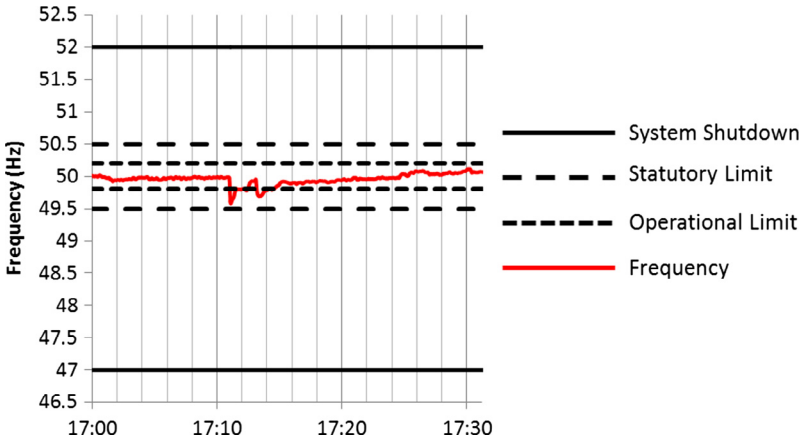

Fig. 1. The statutory and operational frequency limits relative to a real frequency response on the GB system.

FR markets in PJM; New-England; Great Britain; and Germany are compared in [3]. All of these markets are governed by a combination of frequency-based balancing services and slower reserve services. The GB market has a more structured and regulated approach to these services, particularly in the primary frequency regulation category. The Irish transmission system has an extremely high penetration of renewable generation, and is therefore already dealing with frequency issues that will affect larger synchronous power systems in the future. The TSO (Transmission System Operator), Eirgrid, has created the DS3 program [4] to evaluate and develop new system tools, services and policies to manage frequency, among other future network challenges.

ESS have significant operational differences – primarily due to their limited energy capacity – when compared with conventional providers of FR services, such as open cycle gas turbines and pumped hydro storage; it is therefore necessary to design new services to realise the benefits of ESS in maintaining the system frequency. There are research questions arising from the way these services will be designed. In this paper, the following research questions are addressed through a combination of analysis of historical frequency data and experiments using Power Hardware-in-the-Loop (PHIL):

- How quickly can an ESS deliver power in response to a frequency event?
- Can an ESS effectively manage its SoC, therefore ensuring that sufficient energy is available to fulfil its service obligations?
- How does the delivery threshold (deviation from the nominal frequency at which the ESS must respond) affects the service performance, from the perspective of ESS operators and the TSO?
- To what extent can ESS reduce the impact of severe frequency events? How is this power capacity and influenced by the delivery threshold?
- At what SoC should an ESS rest when not providing a service to ensure service delivery while maximising efficiency and minimising battery degradation?
- How can storage be combined with conventional FR providers? And how will new services influence investment in ESS?

The primary contribution of this paper is a methodolgy which can address these questions. The methodology was then used to provide answers for the UK case, and a world leading FR grid service, designed by National Grid, the GB TSO, explicitly for fulfilment by ESS. However, the methods presented here could be used to design frequency services for fulfilment by ESS in power systems throughout the world.

The remainder of this paper is structured as follows: Section 2 contains a review of previous research in which ESS are used for frequency regulation, and a description of a new Enhanced Frequency Response service. Section 3 contains statistical analysis of historical frequency data. In Section 4, new experimental methods are described, which have been devised for evaluating FR services designed for fulfilment by ESS; in Section 5, results and analysis are presented from the GB case study; detailed discussion and suggested avenues for future research are provided in Section 6; finally, conclusions and suggest avenues for future research are explored in Section 7.

2. Background

2.1. Frequency response and energy storage systems

There have been a number of previous studies into the use of ESS to provide FR; the aims, methods, and findings of these studies are summarized in this section. Authors have used modelling approaches ranging from simple transfer functions and integrators [5,6], through to equivalent circuit models [7], and models which attempt to predict system lifetime and battery degradation [7,8].

A variety of ESS technologies have also been evaluated. While lithium ion batteries are the most commonly used storage medium [5,6,9], other modelled technologies include alternative lithium batteries [7], lead-acid, Ni-Cad, NMH, and vanadium redox flow batteries, flywheels [10], super capacitors [9], and superconducting magnets [11]. While there are advantages and disadvantages to each technology, these were all able to provide sufficiently fast responses to provide FR. It is possible that a combination of ESS technologies, or a hybrid of ESS and a conventional or renewable generator, could provide the best compromise; various authors have adopted this approach using virtual power plant techniques [6,7,12].

Although the focus of this paper is regulating the frequency of a large, interconnected transmission system, research on smaller, islanded systems is also relevant. These systems typically have more variable demand and lower inertia than centralized power systems, meaning frequency control is critical. This type of system has also been studied extensively, using a variety of control systems and technologies [9,11,13]. The control approach has been a focus of various studies, including the use of droop control [9,14], control accounting for battery degradation [5,8], and coordinated control between a number of smaller ESS [15,16] or electric vehicles (EVs) [17,18].

FR is typically operated via a service market [3]. There is a compromise in these cases between obtaining the level of service required, and making the service attractive to potential providers. Some studies have investigated FR provision from the perspective of the German and Dutch balancing market operators [10,19]. Some of the conclusions suggested that the power to energy ratio – the stored energy expressed as time at maximum power (P_{max}-·Hrs) – of the ESS technology is significant in ensuring that all contracted services can be fulfilled.

In recent years, a substantial contribution has been made to research on provision of FR via ESS. Knap et al. [20] explore the sizing of ESS for both inertial response and primary frequency response. The presented method employs simulations of the power network and the storage system; a set of droop controllers is used to provide inertia as a function of the ROCOF and primary response as a function of the frequency deviation. The results indicate that, in a system with 50% renewable generation, the required storage capacity is around 5% of the total generation capacity, and the power to energy ratio is approximately 2–1. An alternative to using a conventional ESS is to use a virtual ESS; Cheng et al. [21] use a combination of demand response from domestic refrigerators and flywheel storage to provide primary and secondary frequency response. This system can offer a comparable response to an ESS, but at a significantly reduced cost. Once again, the system is demonstrated via simulation.

It can be seen that ESS can make a contribution to system frequency regulation, and that they can do so more quickly than conventional generation. However, ESS are constrained in terms of energy as well as power, which can prevent them from providing all of their potential benefits to the network.

Considering these constraints, the uptake of ESS for frequency regulation can be facilitated by:

- Design of a service market tailored to the strengths of ESS, with provisions made for their limitations;
- A thorough investigation into the Power to Energy ratio of ESS being used for frequency regulation;
- Laboratory and grid-scale demonstrations of the applications and strategies described – the majority of the research discussed has focused on simulation.

2.2. Enhanced frequency response

In GB, the TSO, National Grid, is responsible for regulating system frequency. At present, this is achieved through the primary, secondary, and high frequency response services: primary response must deliver rated power within 10 s of a low frequency event offering, and maintain the delivery for 30 s; secondary response must provide power within 30 s of a low frequency event and maintain delivery for 30 min; high frequency response combines both services, and foes not have a finite delivery duration. The same provider can offer primary and secondary response, and the power provided to the primary response can carry over to secondary response, as shown in Fig. 2.

National Grid is creating a new internationally leading service to take advantage of the fast response capability of ESS: Enhanced Frequency Response (EFR) [23]. This service is explicitly designed to be delivered by ESS, allowing for state-of-charge (SoC) management between service windows, which was not possible in the existing frequency response services; Fig. 2 shows how EFR interacts with the existing services, while Fig. 3 shows the response curve for EFR. EFR requires the ESS to respond within 1 s of the frequency crossing a threshold, which can be set at ±0.05 Hz or ±0.015 Hz.

National Grid has agreed contracts for 201 MW of EFR capacity, which will include the construction of a 49 MW ESS. However, there is lack of appropriate studies to support the design, validation and optimization of such implementations.

Fig. 3 shows a key feature of EFR, which demonstrates that it has been explicitly designed to be delivered by EESs; an allowance to vary output within ±9% within the frequency deadband. This means that ESS can offer the service continuously i.e. they do not need to commit to SoC adjustment periods with no service. EFR has demanding response requirements, which are well suited to being fulfilled by an ESS:

- Response must take place within 1 s of a frequency deviation occurring.
- The service provider must be able to deliver the service in either direction (export/import to/from grid).
- The service provider must be able to provide 100% capacity for a minimum of 15 min.
- The provider must maintain an operational availability of 95% to qualify for the full payment – availability criteria are shown in Table 1

The service performance measure (SPM) is calculated as the average of the second-by-second ratio of normalized response against the service envelope shown in Fig. 3. The second by second performance measure (SBSPM) is calculated using equation 1 [23]:

$$\begin{aligned} &f < 50, \quad NR > UE \rightarrow SBSPM = \tfrac{UE}{NR} \\ &f < 50, \quad NR < LE \rightarrow SBSPM = \tfrac{NR}{LE} \\ &f > 50, \quad NR > UE \rightarrow SBSPM = \tfrac{NR}{UE} \\ &f > 50, \quad NR < LE \rightarrow SBSPM = \tfrac{LE}{NR} \\ &LE \le NR \le UE \rightarrow SBSPM = 1 \end{aligned} \tag{1}$$

In Eq. (1), F is frequency, LE and UE are the lower and upper envelopes respectively, and NR is the normalized response [23]:

$$NR = \frac{P_t}{P_{max}} \tag{2}$$

where P_t is the response at time t, and P_{max} is the maximum tendered response.

Because EFR is expected to respond more quickly than conventional frequency response, it could cause short-term stability problems without careful management. To avert this, ramp-rate limitations have been included in the service specification. Within the envelope, but outside the deadband, the maximum change in output is limited as a proportion of the rate of change of frequency (ROCOF or $\frac{df}{dt}$). The ramping constant, k, changes with the deadband, as shown in Table 2 [23].

$$P_{max}\left(-\frac{1}{k}\cdot\frac{df}{dt} - 0.01\right) < \frac{dP}{dt} < P_{max}\cdot\left(-\frac{1}{k}\cdot\frac{df}{dt} + 0.01\right) \tag{3}$$

If the service is under-delivering, the maximum ramp rate is given by [23]:

$$0 < \frac{dP}{dt} < \frac{2P\text{max}}{1s} \tag{4}$$

if the service is over-delivering the maximum ramp rate is given by [23]:

$$0 < \frac{dP}{dt} < \frac{0.1P\text{max}}{1s} \tag{5}$$

and within the deadband, the maximum ramp rate is given by [23]:

$$0 < \frac{dP}{dt} < \frac{0.01P\text{max}}{1s} \tag{6}$$

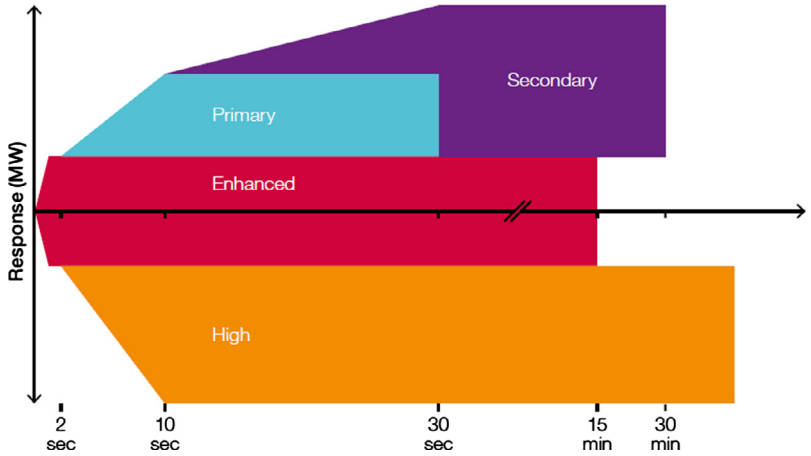

Fig. 2. The available frequency response services in GB, their response times, and their durations [22].

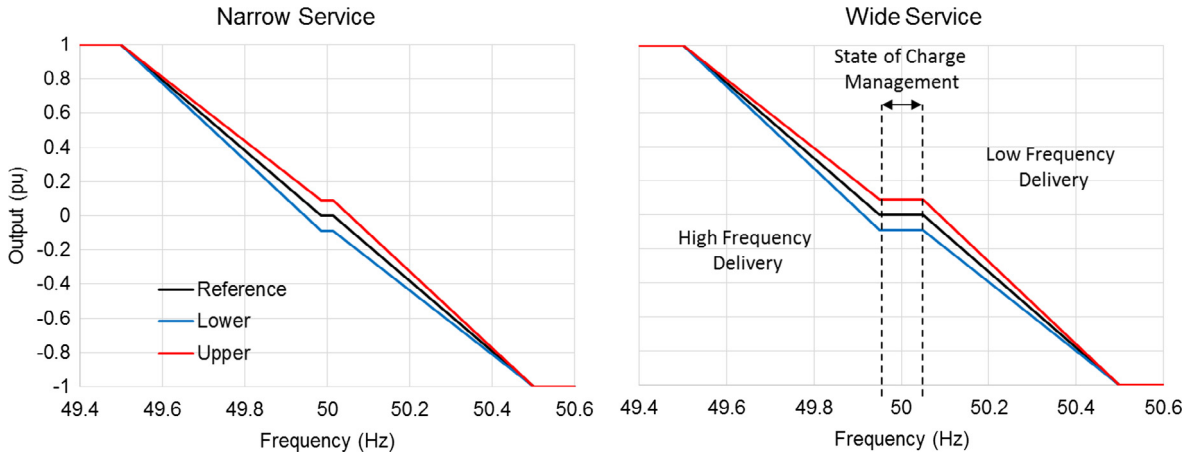

Fig. 3. The response curve for the EFR wide service. The upper and lower bounds show the required power output, as a proportion of the maximum tendered power, for a given frequency. The deadband around 50 Hz allows an ESS to manage its SoC using a proportion of its tendered power [23].

Table 1
Availability criteria for EFR.

Service performance measure (%)	Availability factor (%)
<50	0
≥50, <75	50
≥75, <95	75
≥95	100

Table 2
Wide and narrow service parameters for EFR [23].

Service	Deadband (Hz)	Ramping constant (k)
1 (wide)	50 ± 0.05	0.45
2 (narrow)	50 ± 0.015	0.485

3. Historical frequency data analysis

To allow potential EFR providers to assess the viability of their systems, National Grid have made system frequency data for 2014 and 2015 available at 1 s resolution. This section contains comprehensive analysis of these data to assess the likely operating regime of an ESS providing the EFR services.

Fig. 4 shows that the system frequency is between 49.8 and 50.2 Hz the vast majority of the time – the frequency was out of these bounds just 0.043% of the time. The frequency was within ±0.05 Hz of the nominal value 64% of the time, but within ±0.015 Hz just 19% of the time. The peaks in the frequency histogram are slightly above and below 50 Hz.

3.1. Over- and under-frequency events

The number of over- and under-frequency events is important, because it will determine how often the ESS has to exchange power with the grid. The duration of these events is also significant, because it will determine the depth of discharge. Fig. 5 shows histograms and probability distributions of the number of events per day throughout 2014 and 2015. High frequency events were enumerated by stepping through each day of the data, and counting each time step in which f_t was greater than the service threshold, and f_{t-1} was less than the service threshold; the process was repeated for under-frequency events, and the two were summed to find the total number of events. The average number of events per day for service 1 is 370, with slightly more under-frequency events than over-frequency events; for service 2, this increases to 530 events/day, again with under-frequency events being more common.

While the number of events per day is very high, the majority of those events are very brief; as Fig. 6 shows, around 50% of the events are under 10 s, and less than 10% of events are over

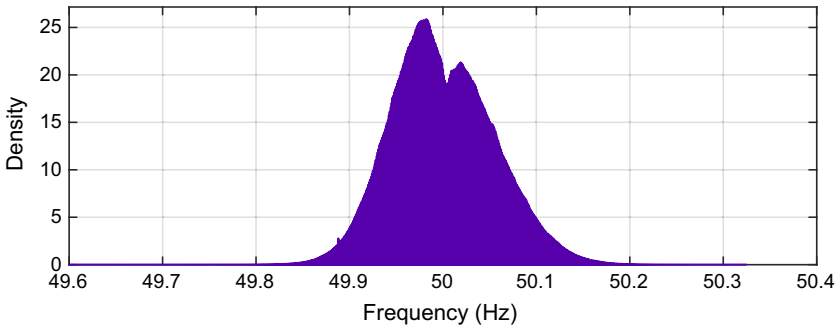

Fig. 4. A histogram of system frequency for 2014 and 2015.

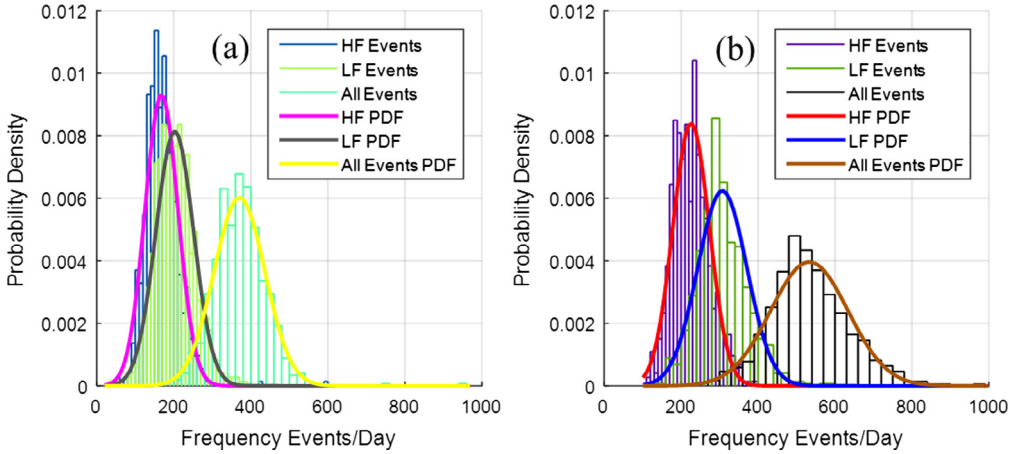

Fig. 5. Histograms and probability distributions of frequency events per day for (a) the wide service and (b) the narrow service.

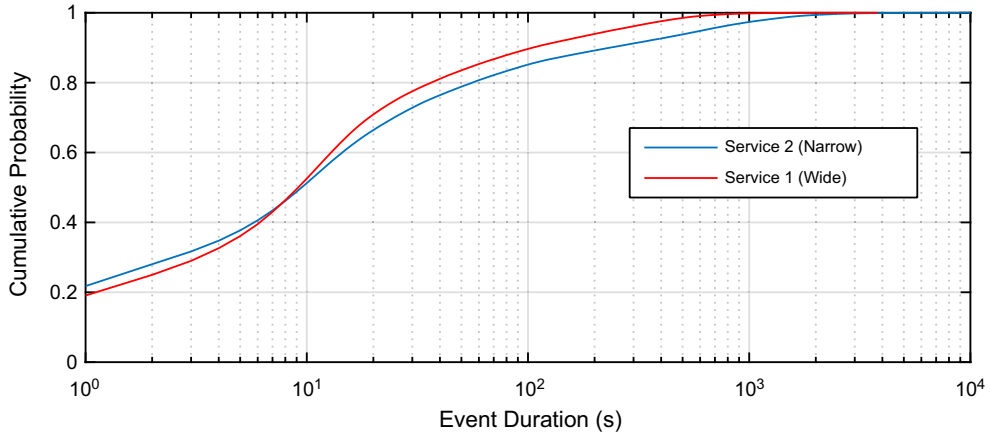

Fig. 6. Cumulative probability distributions of frequency event durations. The duration axis uses a log scale to allow the range of durations to be easily depicted.

2 min. Only 0.26% of service 1 events lasted 15 min or longer – the maximum mandated delivery duration – compared with 3.09% of service 2 events.

3.2. Operating range

The EFR service specification requires the ESS to have sufficient capacity to provide a full power response, in either direction, for 15 min; this requires a minimum capacity of 30 min (0.5 h) at full power. The historical data were used to simulate 2 years of operation for both the wide and narrow services. The SoC was recorded at each timestep. Fig. 7 shows the cumulative probability of deviations from the nominal state of charge for both services. The *x* axis shows the energy in terms of hours spent at maximum power.

When fulfilling the wide service, the SoC range was within −0.0514 and 0.0851 P_{max}·h of the nominal for 99% of the simulated period – this suggests that the mandated ESS is larger than required, and an ESS fulfilling service 1 could operate at an SoC its efficiency and degradation requirements, rather than the service requirements.

When fulfilling the narrow service, the 99% operating range was −0.3969 to 0.4187 P_{max}·h – this implies that the mandated ESS capacity (±0.25 P_{max}·h) would not be sufficient, and that offering

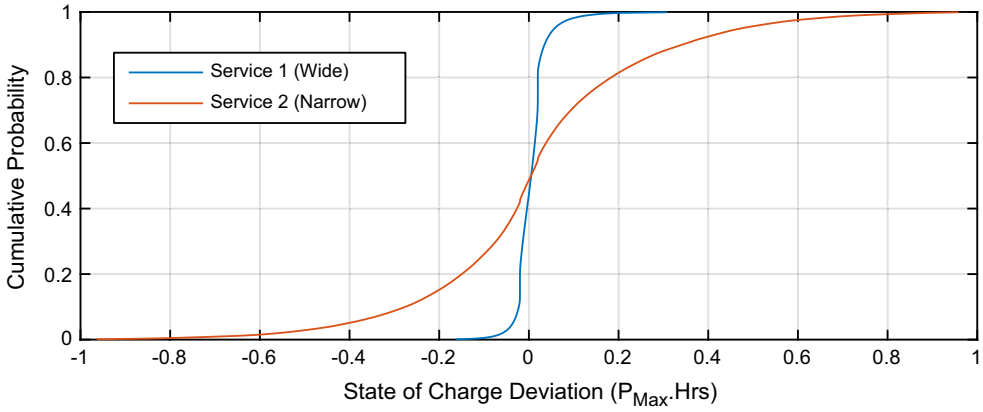

Fig. 7. Cumulative probability curves of swing range for ESS with 1:1 and 2:1 Power:Energy ratios.

service 2 would require additional capital investment to avoid performance penalties.

4. Experimental methods

This section describes the methodology for two experiments designed to inform the development of FR services for ESS; these were designed explicitly to answer the research questions set out in Section 1. The first experiment used high resolution frequency data from the GB system, and was used to evaluate the performance of an ESS responding to real frequency data. The second set made use of large power system model running in real-time, and interacting with the laboratory network and ESS through a Flexible Power Conversion System (FPCS), enabling PHIL, and allowing the authors to observe the impact of the ESS's response on frequency events arising from an imbalance between supply and demand within the model.

4.1. Laboratory setup

The Smart Grid Laboratory at Newcastle University is designed to synergistically combine the scale of simulation with the detail of experimentation. This is achieved through FPCSs, real and emulated ESS, and real-time simulation. A sophisticated ESS emulator is coupled to a 415 V busbar of the laboratory network by a DC/AC power converter, which is controlled via a real-time target computer. The laboratory network itself is energized by an FPCS: a 30 kVA AC/AC converter module, capable of supplying variable voltages and frequencies in real-time. These can be generated from either historical data, such as those described in section III, or a real-time simulated power network. In this way, the actual ESS, network, laboratory based loads and generation, can be virtually connected to larger and more complex networks containing other large loads and generators, and their operation and interaction studied in real-time.

In the experiments presented in this paper, an ESS emulator was used to represent the energy storage medium. This emulator consisted of a programmable DC source, which could be configured to replicate the behaviour of any ESS technology. Its use in this application presents a number of advantages and disadvantages compared to real batteries; it allows logging of otherwise hidden parameters, such as state of charge, and its performance is repeatable, allowing multiple trials to be easily compared. The main disadvantage is that it does not provide a "ramp rate" limitation on the battery technology. However, although EFR requires a fast response in power network terms, this is not a fast response in electrochemical terms, and the rate-limitations come from the power conversion equipment, rather than the battery, which justified the use of an emulator in this case [24]. The emulator was programmed with the characteristics of a Li-Ion battery, with 2 parallel strings of 72 series cells, each with a nominal voltage of 4 V and a capacity of 39 Ah; these parameters were selected based on an ESS demonstration project on the UK distribution network [25]. An illustration of the laboratory set up for these experiments is shown in Fig. 8.

Real-time simulation was carried out using an OPAL-RT real-time simulator [26,27] to model the IEEE 24-bus test network [28]. This technology enabled large power system models to be run in real-time, and allowed the laboratory hardware to operate as though it was coupled to a real transmission-scale network.

The ESS controller, with EFR algorithm, was implemented as a Matlab® script within the Simulink™ model which carried out the low-level control for the DC/AC converter. A feedback loop to manage SoC was also integrated into the overall controller. The frequency was obtained using a phase lock loop process on a voltage waveform measured at the point of common coupling between the AC/DC converter and the laboratory network. This resulted in a small steady state error, which was removed through calibration using measurements from the laboratory network and the AC/AC converter. At each time step, the frequency, ROCOF, previous power set point, and estimated SoC were read in by the controller. If the frequency was within statutory limits, the controller issued a new set point to adjust SoC if necessary. If the frequency was outside the limits, a power set point was calculated using the EFR response curve. In either case, the required power change was checked against the ramp rate limits, and curtailed if necessary. This control algorithm is illustrated, using the parameters for the wide service, in Fig. 9. The controller was calibrated against the ESS efficiency to ensure a symmetric service delivery (that is, the battery current is slightly higher than the service dictates for power to grid services, and slightly lower for power from grid services, due to losses in the converter an the emulated battery internal resistance).

4.2. Power hardware-in-the-loop

One of the key contributions of this paper is demonstrating the capability to provide a real power response to transient events taking place in a real-time simulated power network. PHIL is a technique used to develop and test complex, real-time embedded systems; it enables interfacing of real power hardware with computer models which run in real-time [29]. In this paper, PHIL allows us to conduct experiments as though there is a transmission-scale electrical network in the laboratory, allowing

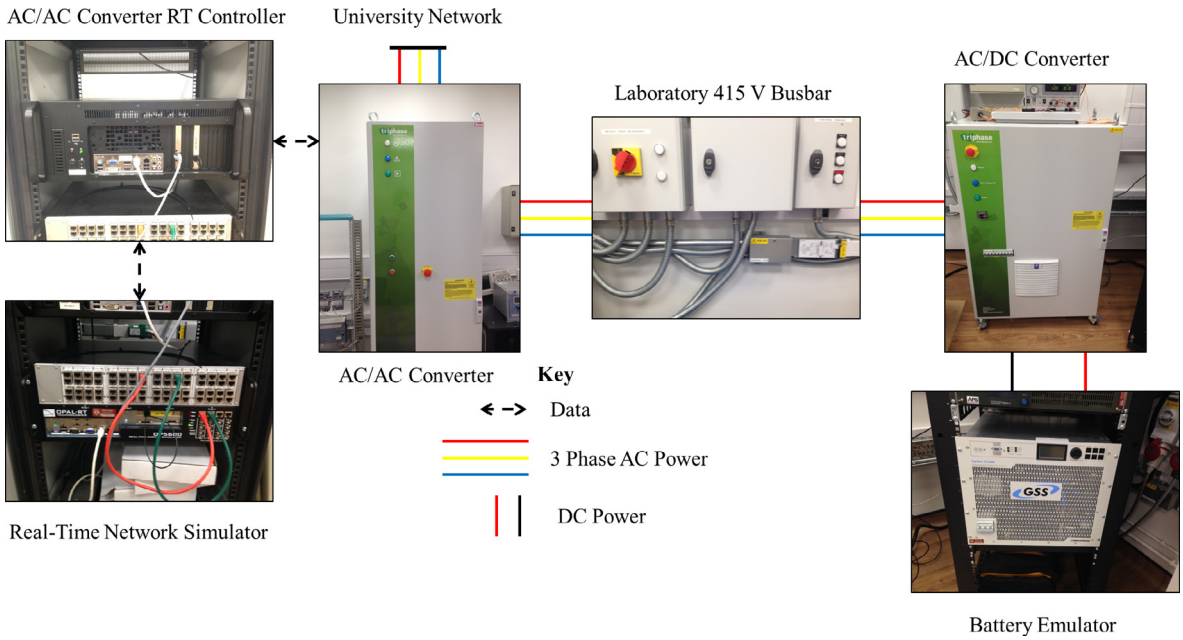

Fig. 8. The laboratory set up for the experiments in this paper, including an illustration of whether the equipment is interaction through AC power, DC power, or data.

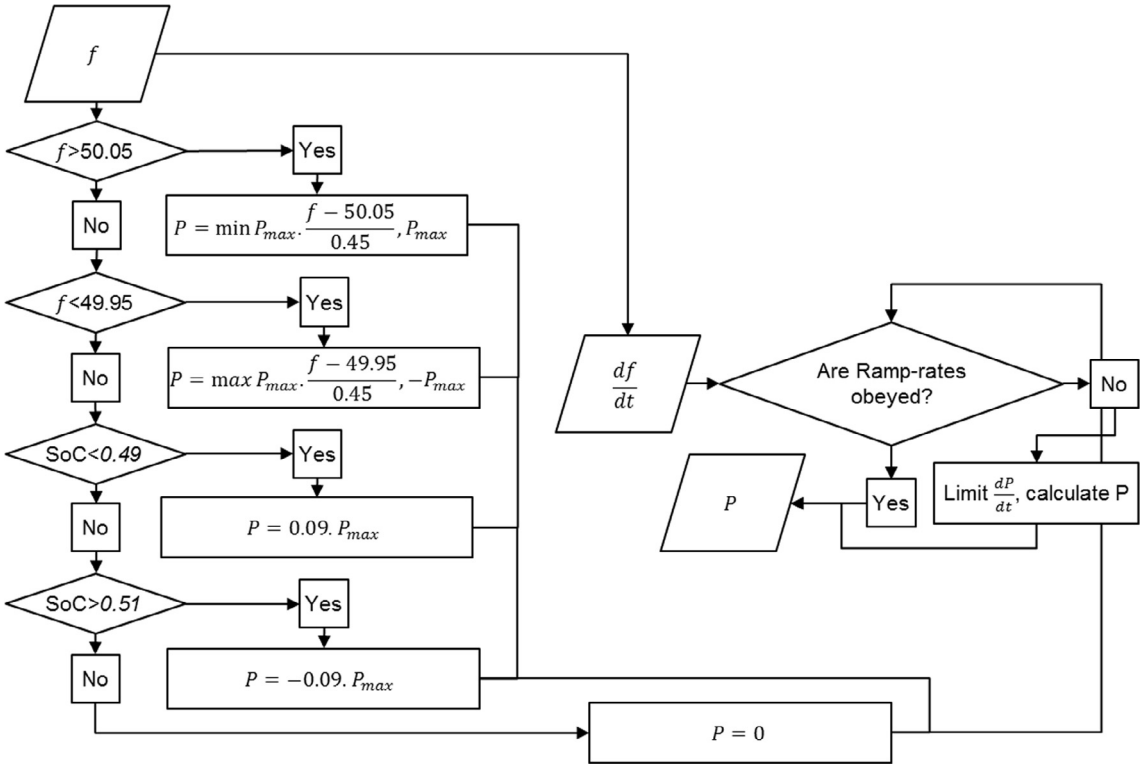

Fig. 9. The control algorithm used for delivering the EFR Wide service, maintaining the SoC between 0.51 and 0.49 when the frequency is within the deadband. The same control can be used, with altered parameters for the narrow service.

us to combine the scale of demonstration projects or simulation with the detail of experimentation. This approach offers advantages over using a simple, inertial model – the full network model will include the impact of network losses, voltage changes, and transient behaviour following a major outage, which can have implications for the siting of the FR provider.

The real-time simulations presented in this paper were conducted using an Opal RT simulator with 4 cores, which enabled simulation of transmission scale networks at a time step of 50 μs; for a simulation to operate in real time, all the calculations need to be complete within the time step to ensure that the results are available for the start of the next time step [30]. The simulated network was partitioned such that each processor completed its allotted calculations in 70–80% of a time step (35–40 μs), and no overruns (an event in which the calculation time exceeds the time step) were reported. The simulations were interfaced to the labora-

tory network via an optical link to a FPCS, which reproduced the voltage and frequency at a specified node on the simulated network onto the physical network. The partitioning of the network and the location of the ESS can be seen in Fig. 10. The ESS was sited at bus 18, where was co-located with a 400 MW generator, and a large demand group (around 250 MVA). The simulation was carried out using the Opal RT Artemis software, which is a re-implementation of the Simulink power systems tool box, optimised for real-time simulations [31]. The complete experimental set up required 3 real-time computations to be conducted simultaneously: one to operate each of the power converters, and a third to carry out the real-time network simulation.

4.3. Experiment I – Responding to historical frequency data

Fig. 11 illustrates the set-up of these experiments. Historical frequency data, as described in Section 3, was used as an input dataset for the FPCSs; this resulted in a varying frequency on the laboratory network. The laboratory ESS then responded to this frequency according to the EFR response curve. Measurements were recorded using transducers at the grid interface of the AC/AC and AC/DC power converters, at a resolution of 20 ms. The experiment was designed to determine experimentally the response time of a real ESS unit, to assess the availability that can be achieved (a measure of accuracy), and to evaluate how the system performance varied between services 1 and 2.

4.4. Experiment II – Response to frequency events using PHIL

A 24-bus test network was simulated in the real-time network simulator at a time step of 50 μs. Frequency events were created by step-changes in demand; the system inertia was set to 3.64×10^8 kg m^2 (Inertia constant, $H = 3.7$ s), and a nominal stored kinetic energy of 17.5 GVAs, such that the resulting frequency deviation would breach the statutory limits (±0.5 Hz). The laboratory ESS responded to the frequency deviation according to the EFR response curve. This experimental setup is illustrated in Fig. 12.

A scaling factor was applied to the resultant power response from the ESS before feeding it into the simulated power system model. This allowed the single ESS in the laboratory to respond as though it was either a large ESS, or many small ESS aggregated together. A set of scaling factors were applied to determine how effective different penetrations of ESS would be at solving frequency deviations.

The purpose of these experiments was to experimentally evaluate how effectively different levels of EFR response can mitigate severe frequency events, and whether there is a significant difference in using Service 1 or 2 to do so.

5. Experimental results

In this section, results are presented from experiments carried out using the methods described in Section 4, the historical fre-

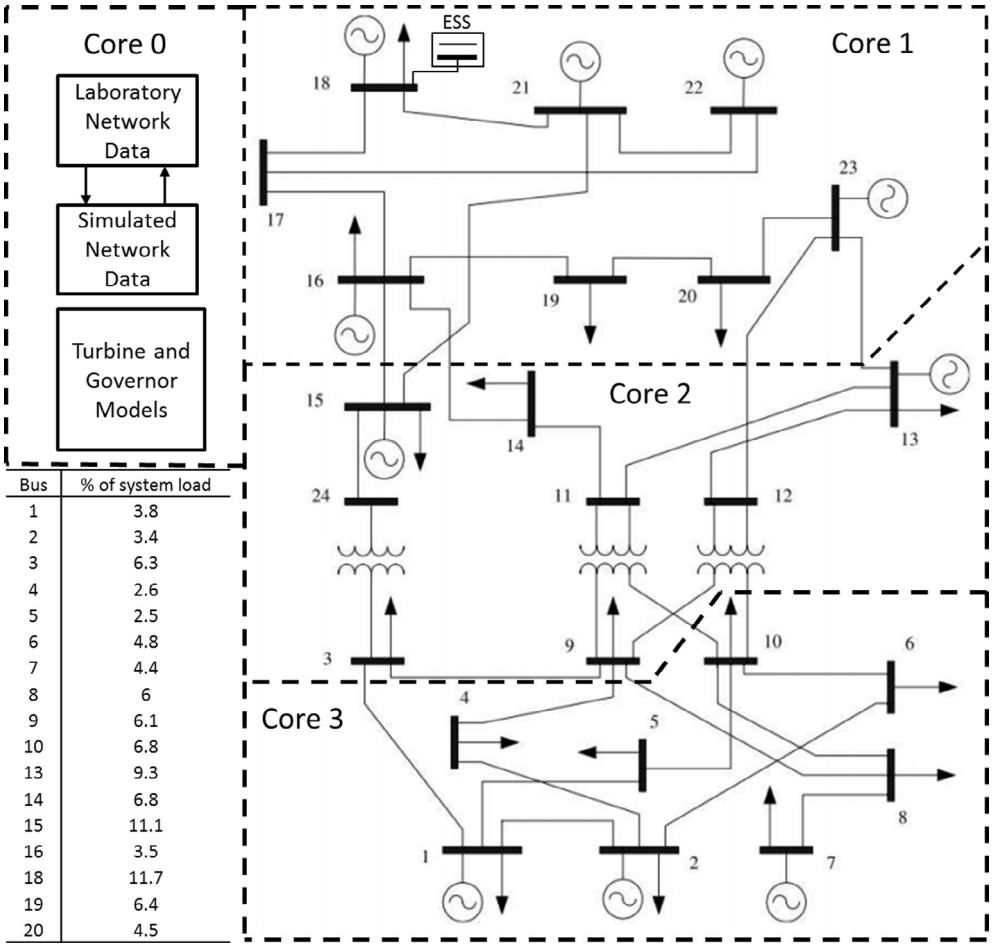

Bus	% of system load
1	3.8
2	3.4
3	6.3
4	2.6
5	2.5
6	4.8
7	4.4
8	6
9	6.1
10	6.8
13	9.3
14	6.8
15	11.1
16	3.5
18	11.7
19	6.4
20	4.5

Fig. 10. The simulated power network, showing how the network was divided between the simulation cores, the connection of the ESS, and the data input to the laboratory network. The network model was built according to data found in [32].

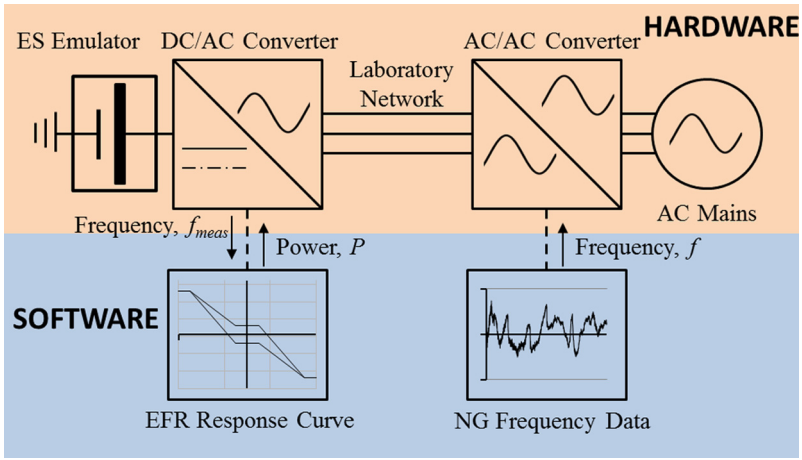

Fig. 11. Experiment I – Responding to historical frequency data – Laboratory and software configuration.

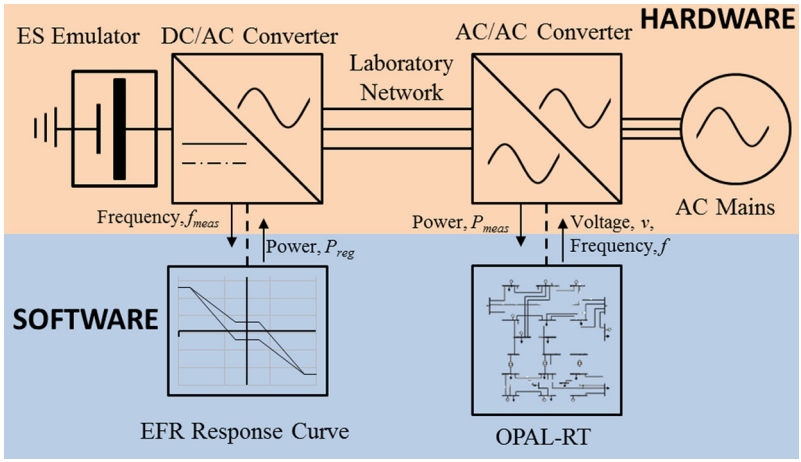

Fig. 12. Experiment II – Response to real-time simulated frequency events – Laboratory and software configuration.

quency data described in Section 3, and the EFR service parameters described in Section 2.2.

5.1. Responding to the historical frequency data

Fig. 13(a) shows that the response from the laboratory ESS satisfied the requirements of both EFR services. When the frequency is out of the frequency deadband, ESS will be triggered to react based on the EFR response curve. Hence, the shown frequency/power plot is corresponds to the response curve for the EFR.

Fig. 13(b) shows time series of power and frequency for the duration of the experiments. The ESS can be seen to react to the changes in frequency. The wide service frequently sits at the ±9% SoC adjustment point while the narrow service is still delivering the service.

Fig. 13(c) shows the SoC of the ESS throughout the experiment. The controller aimed to maintain the SoC between 0.49 and 0.51, and during the experiment the SoC range was 0.5125–0.4771 for the wide service and 0.4184–0.5259 for the narrow service. The results of the experiments and analysis suggest that, for the wide service, the actual operating range is far smaller than the specified operating range. It would be possible in practice to set the operating point below 50% SoC target in order to reduce degradation effects and therefore increase the lifetime of the ESS [33]. However, the narrow service may require more energy capacity than the minimum requirement for the service, due to the lack of opportunities for SoC adjustment.

A cross correlation [34], shown in Fig. 14, was performed on the measured power and the power set point derived from the measured frequency. The maximum correlation occurred with a lag of 4 time steps, which implies a response time of 80 ms; this is significantly shorter than the response time of 1 s required by the EFR specifications. This response could even be quick enough to provide a synthetic inertia service, which is estimated to require a response within 100 ms [35].

5.2. Responding to frequency events in a real-time simulated network

Fig. 15 shows graphs of the frequency and the power response of the energy storage system during a frequency event trigger. A 500 MW imbalance was created within the system, resulting in a substantial drop in frequency. The change in frequency was observed by the ESS in the laboratory, which dispatched power according to the EFR response curve. The experiment was repeated with different scaling factors, corresponding to peak ESS outputs of 50, 100, 250, and 500 MW. As the size of the ESS output increased, the severity of the frequency event was reduced, but the duration of the event was actually slightly increased; this was because a reduced governor response was required, as a result of the action taken by the EFR. The system stayed within the statutory limit (±0.5 Hz) with the 250 MW and 500 MW EFR system.

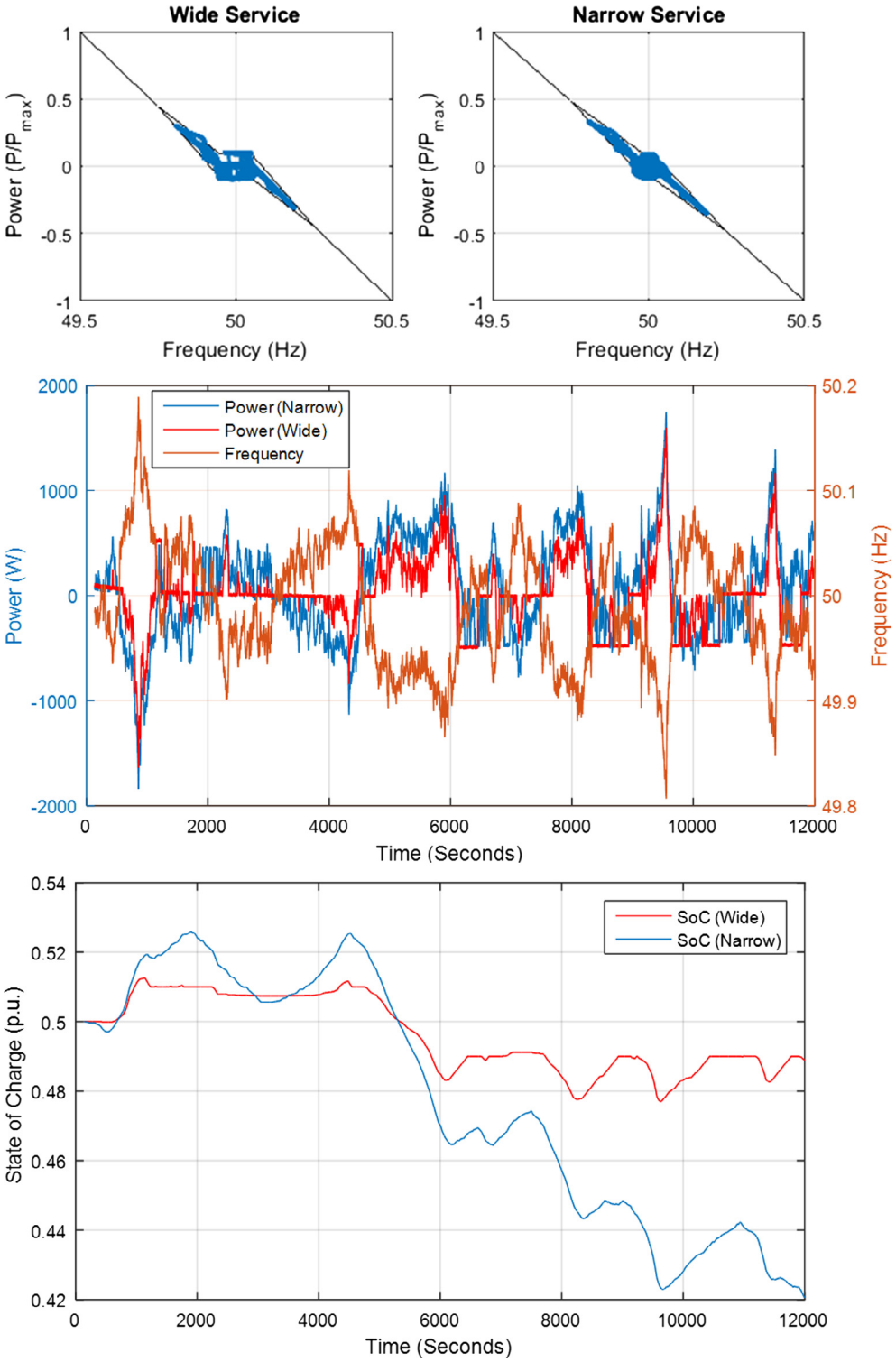

Fig. 13. (a) Power against frequency obtained in response to EFR calls originating from historical data. The response corresponds to the EFR response curve. (b) Plot of frequency and power against time, showing the ESS responding to frequency events. (c) SoC against time, showing that the ESS remains close to 50% throughout its operation.

Given the increased duty, and likely increased energy capacity, required to deliver the narrow service, the results of these experiments have been used to quantify the benefit of delivering the narrow service. Fig. 16 shows the nadir of frequency for each capacity of ESS used during the experiment, and considering both the wide and narrow services. The base case, with no ESS, is also shown. The nadir of frequency is less severe when delivering the narrow service, but only by a small amount, and the change is only pronounced at very high penetrations of EFR.

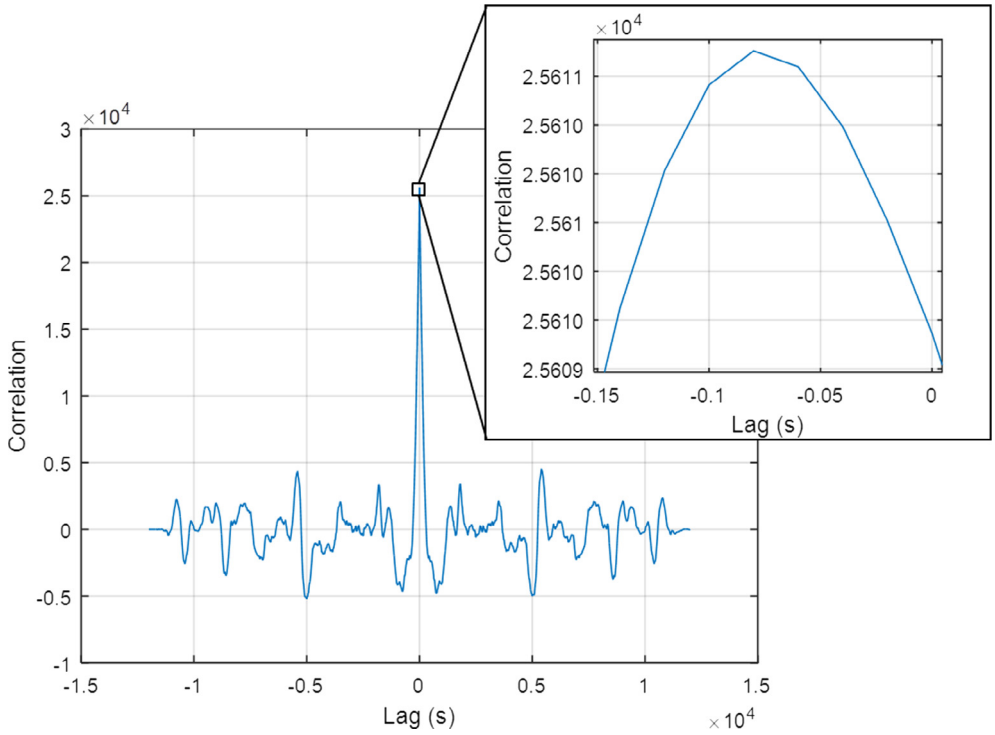

Fig. 14. A plot showing the cross correlation between the power set point inferred from the measured frequency, and measured power.

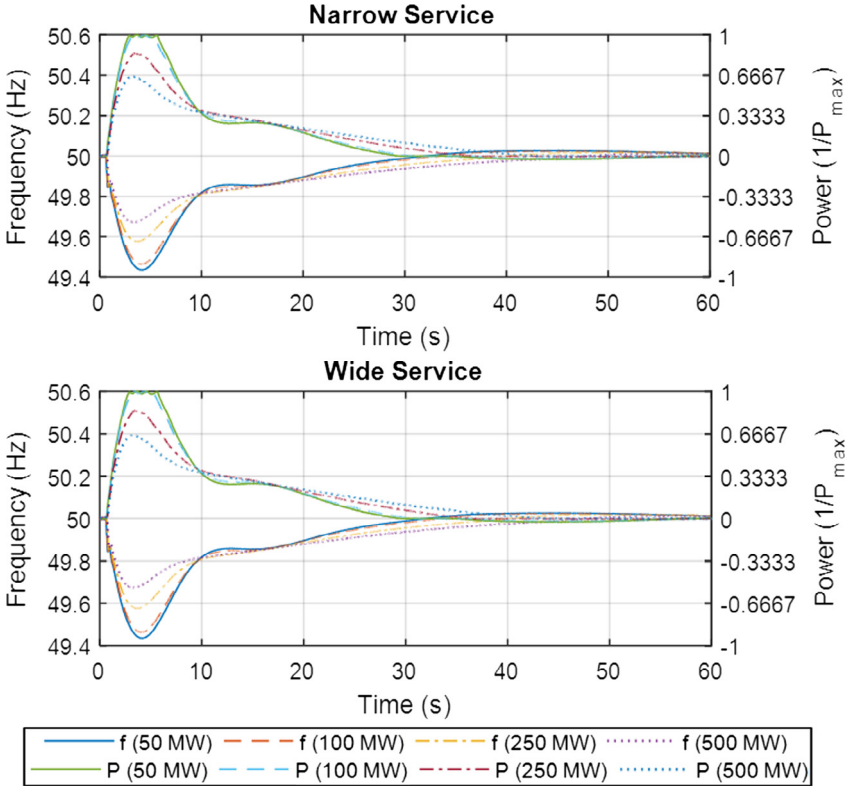

Fig. 15. Deviations in system frequency and resulting ESS response, for ESS ratings of 50–500 MW, performing both the wide and narrow services.

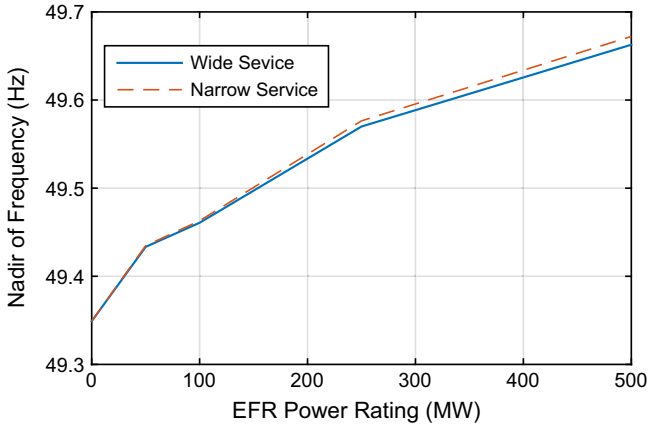

Fig. 16. Comparison of the nadir of frequency between the wide and narrow services.

6. Discussion

In this section, the research questions set out in Section 1 are answered, and avenues for further research, which can build on the methods and results presented in this paper, are discussed.

The results attained using the historical data suggest that the time delay between the frequency crossing the threshold and power being delivered is of the order of 80 ms. This not only suggests that an ESS could deliver EFR, but that an aggregated fleet of ESS, with additional communication latencies, could also meet the service requirements. These experiments, combined with the analysis in section III, also demonstrate that the ESS can manage its SoC while remaining available to deliver the service. The PHIL experiments showed that EFR can reduce the impact of a severe frequency event, reducing the most extreme deviation. However, the results show a diminishing return as additional ESS capacity was installed. Furthermore, while the narrow threshold made a minor improvement to the nadir of frequency for a given ESS power capacity, the results of the statistical analysis suggest this substantially increased the required energy capacity of the ESS.

The EFR service has created a new market for ESS in the UK, which has led to an increase in investment – 201 MW of storage has been contracted, with the largest single ESS rated at 49 MW. However, EFR is designed to be fulfilled continuously, meaning it is unlikely to be delivered in combination with other network services, and it can be delivered from anywhere on the network. These factors suggest that, while EFR will lead to an increase in the number and capacity of ESS on the system, they will not be providing any services to local network operators and will not be located with the provision of such services in mind – effectively being locked-into the provision of EFR. An alternative design, in which the ESS could provide multiple services to TSO and distribution system operators [36–38], could have provided more flexibility for both the network and ESS operators.

The design of services such as EFR could have a profound impact on the design and operation of future power networks, and on which technologies are relied on to provide balancing services. An open-loop response, as is used for EFR, is straightforward for the ESS operator to implement, but will not necessarily offer the best performance for the TSO. The impact of the response from EFR providers will depend on the system inertia, which is not only expected to be much lower in a future power system, but also to vary throughout the day as renewable generation fluctuates [22]. This increases the challenge in designing fast-response balancing and virtual inertia services, because the balancing requirements will continuously be changing, and an over-response could result in rapid system instability. It is possible that a given ESS should be allocated a bespoke frequency response profile, potentially combining a primary and inertial response as described in [20]. An aggregated fleet of smaller ESS, which could comprise domestic storage, EVs, and Virtual ESS, would have even more complex service design requirements, as the available response will be continually changing, the response time will vary across the fleet, and there could be additional latencies arising from necessary communications in such a configuration. Given this, the simple design used for the EFR services is likely to be a first step towards unlocking the potential of these fast-responding, distributed resources. Methods such as those described in this paper are, therefore, essential to test the impact and feasibility of these service designs.

While the methods and results presented in this paper can provide answers to the research questions set out in the introduction, they also represent starting points for future investigations. The methods used here could be used to investigate the effectiveness of various ESS technologies, including storage media such as flywheels, compressed air, and flow batteries, for providing frequency regulation services. The power system model used for the PHIL studies could be enhanced, with variable load groups creating realistic deviations in frequency, similar to those observed in the majority of the historical data. This would allow us to investigate both routine imbalances and extreme events within the same experiment, or investigate adding synthetic inertia [35] to the system. Other future research could focus on combining FR with power flow management and voltage control services.

7. Conclusion

In future power system with reduced system inertia and a high level of variable generation, frequency deviations are likely to become more frequent and more severe. To counteract this, ESS can be used to provide frequency response services in a much shorter timeframe than conventional network assets. However, using ESS in this way presents additional challenges mainly because they are constrained by both energy and power and the fact that their degradation is heavily affected by their operating state of charge and cycling requirements.

In this paper, a new method has been developed to investigate the impact and feasibility of using ESS for frequency response, utilising energy storage emulation, flexible power conversion platforms, real-time simulation, and PHIL. These experimental methods, as well as their results, have archival value and could be adapted to investigate other grid balancing services and low carbon technologies for the perspective of either the TSO or ESS developer. These methods have been demonstrated using the new EFR service which has been designed, from inception, to be delivered by ESS. These techniques have been combined with a novel statistical analysis method utilising high-resolution frequency data from the GB transmission system, yielding a comprehensive understanding of how an ESS providing EFR would operate under the different service regimes.

Our results showed that the ESS had a response time of around 80 ms; this is fast enough that aggregated systems, which could feature additional latency due to communications – are likely to be viable. The two EFR services – with narrow and wide deadbands – were compared. Our findings suggest that the narrow service is technically more challenging, likely requiring four times the storage capacity of the wide service. The narrow service did provide additional benefits, resulting in less severe frequency deviations following a severe demand-generation imbalance, but only by a narrow margin.

The methods presented in this paper can be extended to investigate frequency response services in low inertia systems, includ-

ing more complex service designs or control algorithms, coordination of ESS, demand response, and conventional generation, and combinations of ancillary services offered to both transmission and distribution system operators. The findings can inform future experimental methods, policy, and service design.

Acknowledgements

The work in this paper was funded by the Engineering and Physical Sciences Research Council (EPSRC) under grant number EP/K002252/1, and the Newton Fund under grant number 172733856. The authors would also like to thank Martin Feeney, Smart Grid Lab Supervisor, for his help with the experimental work described in this paper.

References

[1] Weedy BM. Electric power systems. John Wiley & Sons Inc; 2012.
[2] Ulbig A, Borsche TS, Andersson G. Impact of low rotational inertia on power system stability and operation. IFAC Proc Vol 2014;47:7290–7.
[3] Pandurangan V, Zareipour H, Malik O. Frequency regulation services: a comparative study of select North American and European reserve markets North American power symposium (NAPS); 2012.
[4] Eirgrid. The DS3 programme: delivering a secure, sustainable electricity system; 2016.
[5] Stroe DI, Knap V, Swierczynski M, Stroe AI, Teodorescu R. Suggested operation of grid-connected lithium-ion battery energy storage system for primary frequency regulation: Lifetime perspective. In: IEEE energy conversion congress and exposition (ECCE). p. 1105–11.
[6] Swierczynski M, Stroe DI, Stan AI, Teodorescu R. Primary frequency regulation with Li-ion battery energy storage system: A case study for Denmark. In: ECCE Asia Downunder (ECCE Asia). IEEE; 2013. p. 487–92.
[7] Swierczynski M, Stroe DI, Stan AI, Teodorescu R, Sauer DU. Selection and performance-degradation modeling of $LiMO_2/Li_4Ti_5O_{12}$ and $LiFePO_4$/C battery cells as suitable energy storage systems for grid integration with wind power plants: an example for the primary frequency regulation service. IEEE Trans Sustain Energy 2014;5:90–101.
[8] Thorbergsson E, Knap V, Swierczynski M, Stroe D, Teodorescu R. Primary frequency regulation with li-ion battery based energy storage system – evaluation and comparison of different control strategies. In: Proceedings of the 35th international telecommunications energy conference 'smart power and efficiency' (INTELEC), Hamburg, Germany; 2013.
[9] Mongkoltanatas J, Riu D, LePivert X. Energy storage design for primary frequency control for islanding micro grid. In: IECON 2012 – 38th annual conference on IEEE industrial electronics society. p. 5643–9.
[10] Zhang F, Tokombayev M, Song Y, Gross G. Effective flywheel energy storage (FES) offer strategies for frequency regulation service provision. In: Power Systems Computation Conference (PSCC). p. 1–7.
[11] Indu PS, Jayan MV. Frequency regulation of an isolated hybrid power system with superconducting magnetic energy storage. In: 2015 International conference on power, instrumentation, control and computing (PICC). p. 1–6.
[12] Leitermann O, Kirtley JL. Energy storage for use in load frequency control. In: IEEE conference on innovative technologies for an efficient and reliable electricity supply (CITRES). p. 292–6.
[13] Delille G, Francois B, Malarange G. Dynamic frequency control support by energy storage to reduce the impact of wind and solar generation on isolated power system's inertia. IEEE Trans Sustain Energy 2012;3:931–9.
[14] Li X, Huang Y, Huang J, Tan S, Wang M, Xu T, et al. Modeling and control strategy of battery energy storage system for primary frequency regulation. In: International conference on power system technology (POWERCON). p. 543–9.
[15] Chen H, Ye R, Wang X, Lu R. Cooperative control of power system load and frequency by using differential games. IEEE Trans Control Syst Technol 2015;23:882–97.
[16] Sang-Ji L, Jin-Young C, Dong-Jun W, In-Sun C, Geon-Ho A, Yeong-Jun C. In: Frequency control of energy storage system based on hierarchical cluster structure. Eindhoven: IEEE; 2015. p. 1–5.
[17] Ko K, Han S, Sung DK. Performance-based settlement of frequency regulation for electric vehicle aggregators. IEEE Trans Smart Grid 2016. pp. 1–1.
[18] Mu Y, Wu J, Ekanayake J, Jenkins N, Jia H. Primary frequency response from electric vehicles in the Great Britain power system. IEEE Trans Smart Grid 2013;4:1142–50.
[19] Strassheim A, Haan JESD, Gibescu M, Kling Strassheim WL. Provision of frequency restoration reserves by possible energy storage systems in Germany and the Netherlands. In: 11th international conference on the European energy market (EEM14). p. 1–5.
[20] Knap V, Chaudhary SK, Stroe DI, Swierczynski M, Craciun BI, Teodorescu R. Sizing of an energy storage system for grid inertial response and primary frequency reserve. IEEE Trans Power Syst 2016;31:3447–56.
[21] Cheng M, Sami SS, Wu J. Benefits of using virtual energy storage system for power system frequency response. Appl Energy 2017;194:376–85.
[22] National Grid. System operability framework; 2016.
[23] National Grid. Enhanced frequency response; 2016. Available: http://www2.nationalgrid.com/Enhanced-Frequency-Response.aspx
[24] Lijun G, Shengyi L, Dougal RA. Dynamic lithium-ion battery model for system simulation. IEEE Trans Compon Packag Technol 2002;25:495–505.
[25] Lang P, Wade N, Taylor P, Jones P, Larsson T. Early findings of an energy storage practical demonstration. 21st internantional conf and exhibition on electricity distribution, Frankfurt, Germany; 2011.
[26] Bian D, Kuzlu M, Pipattanasomporn M, Rahman S, Wu Y. Real-time co-simulation platform using OPAL-RT and OPNET for analyzing smart grid performance. In: IEEE power & energy society general meeting. p. 1–5.
[27] Singh SK, Padhy BP, Chakrabarti S, Singh SN, Kolwalkar A, Kelapure SM. Development of dynamic test cases in OPAL-RT real-time power system simulator. In: Eighteenth National Power Systems Conference (NPSC). p. 1–6.
[28] Reliability test system task force. The IEEE reliability test system-1996. IEEE Trans Power Syst 1999;14:1010–20.
[29] Guillaud X, Faruque MO, Teninge A, Hariri AH, Vanfretti L, Paolone M, et al. Applications of real-time simulation technologies in power and energy systems. IEEE Power Energy Technol Syst J 2015;2:103–15.
[30] Belanger J, Venne P, Paquin JN. The what, where and why of real-time simulation. Planet RT 2010;1:25–9.
[31] Dufour C, Saad H, Mahseredjian J, Bélanger J. Custom-coded models in the state space nodal solver of ARTEMiS. In: Proceeding of the 2013 International Conference on Power System Transients (IPST-2013); 2013.
[32] Ordoudis C, Pinson P, Morales JM, Zugno M. An updated version of the IEEE RTS 24-bus system for electricity market and power system operation studies. Technical University of Denmark; 2016.
[33] Patsios C, Wu B, Chatzinikolaou E, Rogers DJ, Wade N, Brandon NP, et al. An integrated approach for the analysis and control of grid connected energy storage systems. J Energy Storage 2016;5:48–61.
[34] Knapp C, Carter G. The generalized correlation method for estimation of time delay. IEEE Trans Acoust Speech Signal Process 1976;24:320–7.
[35] EIERGRID and SONI. Phase 2 study report: RoCoF alternative & complementary solutions project; 2016.
[36] Greenwood D, Wade N, Papadopoulos P, Heyward N, Mehtah P, Taylor P. Scheduling power and energy resources on the smarter network storage project. Presented at the 23rd int 2015 conf and exhibition on electricity distribution, Lyon, France; 2015.
[37] Greenwood D, Wade N, Taylor P, Papadopoulos P, Heyward N. A probabilistic method combining electrical energy storage and real-time thermal ratings to defer network reinforcement. IEEE Trans Sustain Energy 2017;8:374–84.
[38] Moreno R, Moreira R, Strbac G. Appl Energy 2015;137:554–66.